Chemical Engineering Journal 101 (2004) 49–56

Chemical Engineering Journal

www.elsevier.com/locate/cej

Analysis of a toluene stripping process: a comparison between a microfabricated stripping column and a conventional packed tower

Stephen H. Cypes, J.R. Engstrom*

School of Chemical and Biomolecular Engineering, 120 Olin Hall, Cornell University, Ithaca, NY 14853, USA

Received 29 July 2003; accepted 13 October 2003

Abstract

Toluene, a volatile organic compound (VOC), was removed from water using a stripping process in both a traditional randomly packed tower and a microfabricated stripping column (MFSC). The MFSC, fabricated using standard Si processing techniques, resulted in overall capacity coefficients, $K_x a$, nearly an *order of magnitude* greater than the packed tower. This increase is a result of less resistance to mass transfer in the liquid phase due to the reduced thickness of the liquid film that is intrinsic to the design of the device. Experimental data from both the packed tower and the MFSC were in good agreement with both the Onda and Sherwood correlations, e.g., the MFSC followed a power-law relationship with respect to $K_x a$ versus flowrate, a result expected for convective mass transfer processes.

Keywords: Microreactor; Stripping; VOC; Absorption; Toluene

1. Introduction

The past decade has shown significant advancements in the field of microreaction engineering, which has produced microfabricated devices capable of handling traditional unit operations on a microscopic scale. The inherently small size of the devices results in the ability to achieve large temperature or concentration gradients resulting in more efficient heat and mass transfer. These features also permit safer methods to handle toxic compounds or dangerous reactions [1]. Only recently, however, have microfluidic units appeared that are capable of handling gas/liquid reactions. Most of these devices were fabricated in order to better control potentially dangerous exothermic reactions such as hydrogenations or fluorinations [2–5]. Most important to the study we report here, there are recent examples of investigations of more traditional unit operations such as absorption, stripping, and extraction in microfluidic devices that contact a gas phase with a liquid phase [6,7].

In this paper, we will describe the fabrication of a microfluidic device capable of handling many unit operations requiring a gas/liquid interface. We will then present results on the ability of this unit to remove trace toluene from water via a convective mass transfer stripping process with dry nitrogen. It will also be shown that the underlying mass transfer coefficients that describe the rate of toluene removal are nearly *an order of magnitude greater* in the microfabricated stripping column (MFSC) as compared to a conventional packed tower.

2. Experimental

The microfabricated stripping column was fabricated from Si using standard Si processing techniques, using 100 mm wafers. Fig. 1 shows a schematic of the process used to fabricate the device, and the device is shown in a perspective that is looking in the direction of the flow. The MFSC is fabricated beginning with two double-side polished Si wafers coated with 150 nm of low-pressure chemical vapor deposition (LPCVD) nitride. Both of these wafers have flow channels and inlets/outlets patterned using standard photolithography. The nitride layers, which act as the masks for the KOH etching step, are etched using a CF_4 plasma. The channels are then etched into the silicon using a timed KOH anisotropic etch. The wafer to be bonded on top, labeled as the "Liquid-side wafer," is then coated on both sides with plasma-enhanced chemical vapor deposition (PECVD) oxide. Perforations that will serve as the contact region between the gas and liquid phases are patterned onto the backside of this wafer, the oxide is etched with CHF_3/O_2 plasma, and the nitride is etched with CF_4 plasma. The perforations are then etched through the silicon, stopping at the frontside oxide

* Corresponding author. Tel.: +1-607-255-9934; fax: +1-607-255-9166.
E-mail address: jre7@cornell.edu (J.R. Engstrom).

1385-8947/$ – see front matter © 2004 Elsevier B.V. All rights reserved.
doi:10.1016/j.cej.2003.10.014

Nomenclature

a	interfacial area for mass transfer per unit volume ($m^2\,m^{-3}$)
A	cross-sectional area of stripper (cm^2)
$C_{A,L}$, $C_{A,I}$	concentration of species A in the bulk liquid and at the interface, respectively ($mol\,cm^{-3}$)
g	gravitational constant ($m\,s^{-2}$)
G_x, G_y	liquid and gas mass flux, respectively ($g\,cm^{-2}\,min^{-1}$)
H	Henry's constant, based on mole fractions (dimensionless)
H_{ox}	height of each theoretical transfer unit (cm)
J	molar rate of mass transfer ($mol\,cm^{-3}\,min^{-1}$)
k_x, k_y	convective mass transfer coefficient in the liquid and gas, respectively ($mol\,cm^{-2}\,min^{-1}$)
K_x	overall convective mass transfer coefficient, based on the liquid mole fraction ($mol\,cm^{-2}\,min^{-1}$)
K_xa	overall capacity coefficient, based on the liquid mole fraction ($mol\,cm^{-3}\,min^{-1}$)
L	molar liquid flowrate ($mol\,min^{-1}$)
N_A	molar flux of species A from the liquid into the gas ($mol\,cm^{-2}\,min^{-1}$)
N_{ox}	number of theoretical transfer units obtained (dimensionless)
$P_{A,G}$, $P_{A,I}$	partial pressure of species A in the bulk gas and at the interface, respectively (atm)
Q_L, Q_G	volumetric flowrate of liquid and gas in packed tower, respectively ($cm^3\,min^{-1}$)
S	defined as $(HV)/L$ (dimensionless)
U_0	superficial liquid velocity ($cm\,min^{-1}$)
$\langle v_L \rangle$	average liquid velocity ($cm\,min^{-1}$)
V	molar gas flowrate ($mol\,min^{-1}$)
$V_{f,L}$	volume fraction liquid in packed tower (dimensionless)
X_a, X_b	mole fraction of toluene at the inlet and outlet of stripper, respectively (dimensionless)
X_A, $X_{A,I}$	mole fraction of species A in the bulk liquid and at the interface, respectively (dimensionless)
X_A^*	mole fraction of species A in equilibrium with Y_A (dimensionless)
Y_A, $Y_{A,I}$	mole fraction of species A in the bulk gas and at the interface, respectively (dimensionless)
Z	height of packed tower or length of MFSC (cm)

Greek letters

δ	liquid film thickness (cm)
μ	liquid film viscosity (Pa s)
ρ	liquid film density ($g\,cm^{-3}$)

layer, using the Bosch etch process. The oxide and nitride layers are removed using concentrated HF at room temperature. After the first KOH etch on the "Gas-side wafer," the nitride is removed using concentrated HF at room temperature. 6.5 nm of chrome is then thermally evaporated onto the frontside of the wafer to act as an adhesion layer, followed by 150 nm of gold. The backside of the Liquid-side wafer is contacted to the frontside of the Gas-side wafer, and the stack is heated to 425 °C with a piston force of 1000 N for 30 min. This process bonds the two wafers via Au–Si eutetic bonding. After bonding the two Si wafers, a Pyrex® (Corning code 7740) wafer is placed on the frontside of the Liquid-side wafer and is anodically bonded to complete the MFSC.

Fig. 2 shows a cross-section of the final device with a scanning electron microscope (SEM) image showing the top of the liquid channel and the perforations that contact the gas channel. The final dimensions of the liquid and gas microchannels are approximately 3.35 cm long × 920 (450) μm wide at the top (bottom) × 330 μm deep. The completed device is mounted on a custom-designed stainless-steel platform (cf. Fig. 3) where the microfluidic interface is provided by spring-loaded o-ring seals (Viton, size #007). Each completed set of devices gives eight parallel sets of channels that are separated by 8.98 mm. The microfluidic platform is designed to interface with four of the eight channels at one time (a 180° rotation of the device accesses the other four channels).

In order to evaluate the performance of the device, we have examined the stripping of toluene from water. Water saturated with toluene (Aldrich) at room temperature is introduced into the liquid channel using a precision syringe pump (Harvard PHD 2000), while dry N_2 flows countercurrently in the gas channel using a gas cylinder (Airgas) controlled with a pressure regulator and a rotameter (Omega FL-3841ST). Fig. 3 shows a simplified schematic of the experimental setup for the characterization of the MFSC, a photograph of the stainless-steel microfluidic interface, and a schematic cross-section of the MFSC and the interface. To form a point of comparison to the MFSC, a conventional packed tower was also used to strip toluene from water. A packed tower forms a reasonable point of

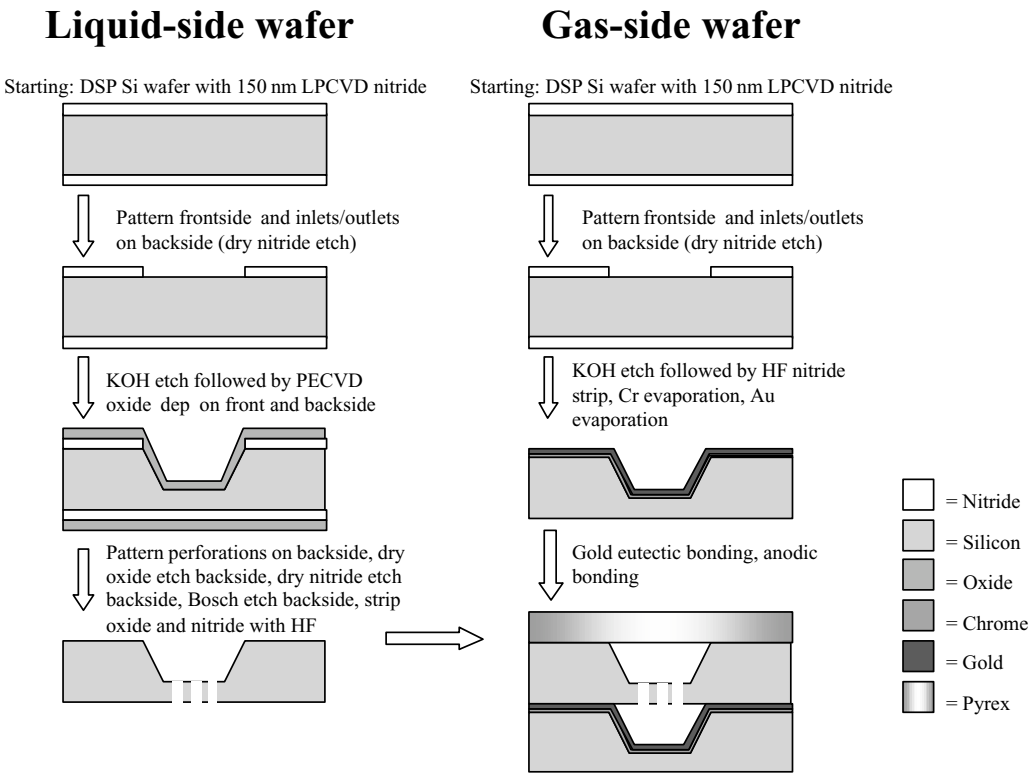

Fig. 1. Process flow diagram for the fabrication of the MFSC.

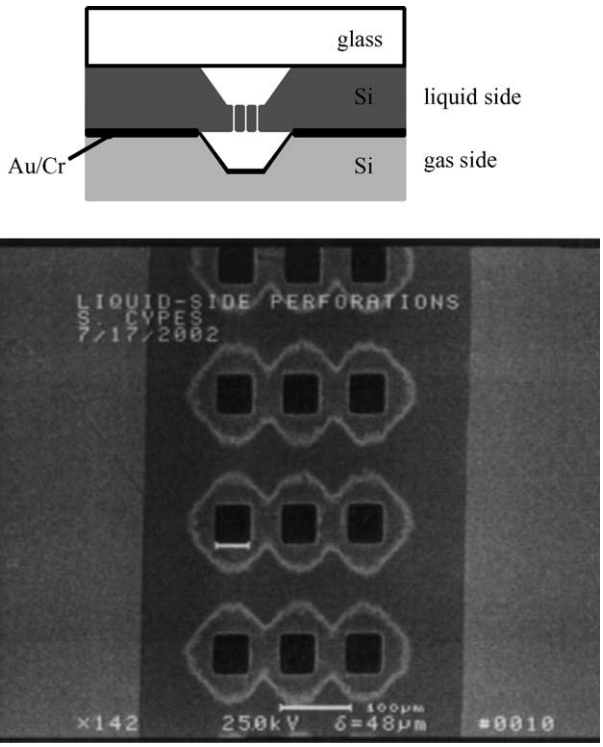

Fig. 2. Cross-sectional schematic of the MFSC, and an SEM image of the liquid channel showing a "top view" of the perforations that contact the gas channel. Non-ideal "footing" of the Bosch etch produced the circular features about each perforation. The channel in the actual device contains 140 rows of three perforations per row.

comparison for this process since, for wastewater treatment, stripping processes are almost exclusively performed using randomly packed towers. A 18.3 cm i.d. column was packed with 114 cm of 1.59 cm plastic Pall rings. Water essentially saturated with toluene was stirred continuously in a tank and pumped through a rotameter to the top of the packed tower. Dry air was passed through a separate rotameter to the bottom of the packed tower, resulting in counter-current flow with the liquid cascading down the tower. Fig. 4 shows a simplified schematic of the experimental setup of the packed tower. All toluene concentrations in water were determined using a gas chromatograph (GC). The GC was calibrated by saturating water with toluene at room temperature, obtaining toluene solubility data as a function of temperature [8], and using this solution as a standard.

3. Results and discussion

Stripping is a common unit operation performed in many industries to remove volatile components from a liquid stream into a gas stream. The rate of removal of the volatile compound can be described by two-phase film theory. Fig. 5 shows a schematic of the relative concentrations of a volatile compound, species A, in each of the phases. At steady-state, the flux of species A through the gas must equal the flux through the liquid. This relationship is given

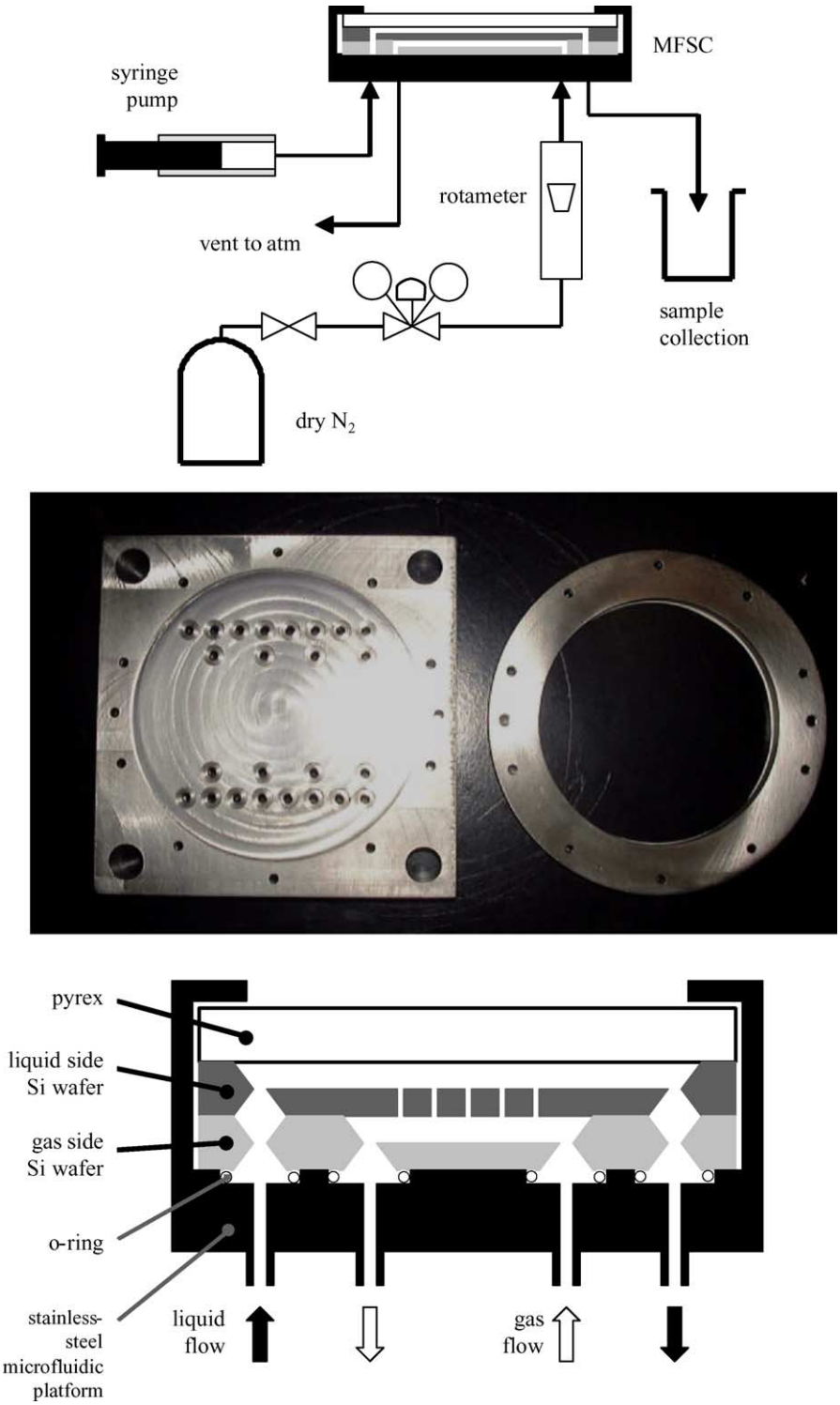

Fig. 3. Schematic of the experimental setup of the MFSC for the stripping of toluene from water using dry nitrogen. Also shown is a photograph of the stainless-steel microfluidic interface, and a cross-sectional schematic of the MFSC and the interface.

in the following equation:

$$N_A = k_x(X_A - X_{A,I}) = k_y(Y_{A,I} - Y_A) \quad (1)$$

Since it is very difficult to measure the interfacial concentrations of a species, an overall mass transfer coefficient can be defined to take into account resistances to mass transfer in both the liquid and gas phases. Through a series of steady-state relationships similar to Eq. (1), the resulting form for K_x, the overall mass transfer coefficient, can be determined [9], and is given in the following

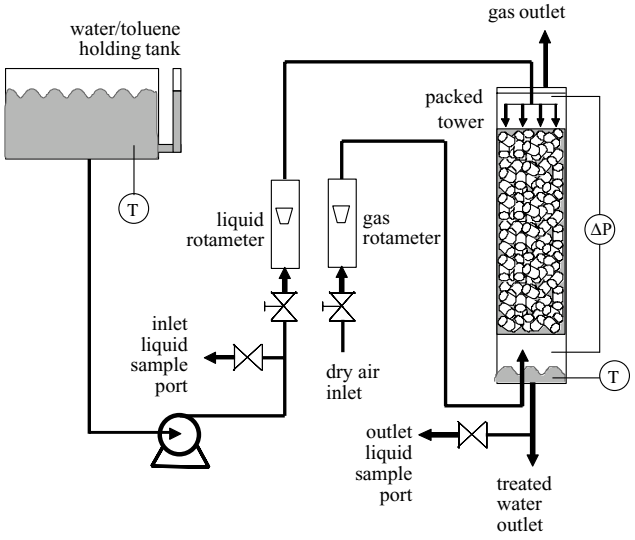

Fig. 4. Schematic of the experimental setup of the packed tower for the stripping of toluene from water using dry air.

equation:

$$\frac{1}{K_x} = \frac{1}{k_x} + \frac{1}{Hk_y} \tag{2}$$

The total rate of mass transfer also depends on the gas/liquid interfacial area. Since it is often difficult to measure the total surface area available for mass transfer, e.g., when using random packings in a packed tower, an overall capacity coefficient is typically defined. If the surface area per volume available for mass transfer is a, then the overall capacity coefficient is given by, $K_x a$. The rate that species A is removed from the liquid to the gas can then be written in terms of the bulk mole fraction of species A in each phase as given by the following equation:

$$J = K_x a(X_A^* - X_A) \tag{3}$$

To experimentally determine $K_x a$ when the inlet and outlet mole fractions of species A are known, Eqs. (4)–(6) can be used [10]:

$$Z = H_{ox} N_{ox} \tag{4}$$

$$N_{ox} = \frac{S}{S-1} \ln \frac{(X_a/X_b)(S-1)+1}{S} \tag{5}$$

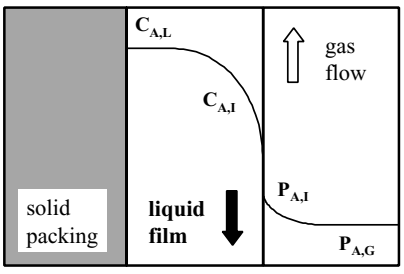

Fig. 5. Relative concentration of a volatile species stripped from a liquid phase into a gaseous phase.

$$H_{ox} = \frac{Z}{N_{ox}} = \frac{L}{AK_x a} \tag{6}$$

and $S = HV/L$.

There have been a number of semi-empirical models published that attempt to predict the overall capacity coefficient for packed towers [11–15]. These models take into account variables such as gas and liquid flowrates, packing type and size, and physical properties such as viscosities, densities, and diffusion coefficients. In most of these correlations the overall capacity coefficient is related to the gas and liquid flow rates by a power-law equation. This is to be expected since convective mass transfer processes result in mass transfer coefficients that vary as the Reynolds number to some power. Therefore, it should also be expected that the data for the MFSC and packed tower should follow a power-law relationship, such as that given by

$$K_x a = \psi G_x^{\alpha} G_y^{\beta} \tag{7}$$

To determine the parameters α, β and ψ for each process, a series of experiments were carried out at different values of G_x and G_y, and $K_x a$ was calculated for these experiments using Eqs. (4)–(6). For the MFSC, G_x and G_y were varied over the range: $G_x \sim 8$–$380\,\mathrm{g\,cm^{-2}\,min^{-1}}$, and $G_y \sim 14$–$59\,\mathrm{g\,cm^{-2}\,min^{-1}}$. For the packed tower the ranges were: $G_x \sim 16$–$80\,\mathrm{g\,cm^{-2}\,min^{-1}}$, and $G_y \sim 1$–$5.6\,\mathrm{g\,cm^{-2}\,min^{-1}}$. The gas mass flux tested in the packed tower was substantially less than the MFSC since the packed tower is limited by flooding conditions. For the MFSC, *Re* for the liquid side ranged from 0.6 to 30.6 for these values of G_x. For these cases, *Re* was calculated assuming the density and viscosity of the solution was equal to that of pure water at room temperature. For a dimension characterizing the flow we used a hydraulic diameter, D_H, equal to (4 × cross-sectional area)/wetted perimeter. For our microchannel, we found that $D_H = 415\,\mu\mathrm{m}$. Briefly we found that the number of theoretical transfer units (N_{ox}) were greater in most trials for the packed tower—this is almost certainly due to the fact that the height of a transfer unit (H_{ox}) is substantially greater in the packed tower as compared to the MFSC. Focusing on the overall capacity coefficients, $K_x a$, however, we found that these were nearly an order of magnitude greater for the MFSC as compared to the packed tower. An example of this is displayed in Fig. 6, where we plot $K_x a$ versus the liquid mass flux, G_x, for both the MFSC and the packed tower. The different symbols for the MFSC data represent four different fixed values for the gas mass flux, G_y. As may be seen, the liquid mass flux has a strong influence on the capacity coefficient. If the data for the MFSC are fit to a power law (at fixed values of G_y), exponents ranging from $\alpha = 0.63$ to 1.0 are found. A fit of the combined data (valid if $\beta \sim 0$) gives $\alpha = 0.84$ for the MFSC. The data for the packed tower are also well described by the power law, and a fit to the entire data set gives $\alpha = 0.72$. To better display the effect of the gas mass flux, we plot the quantity $K_x a / G_x^{\alpha}$ versus G_y in Fig. 7 for both the MFSC and the packed tower. As may be

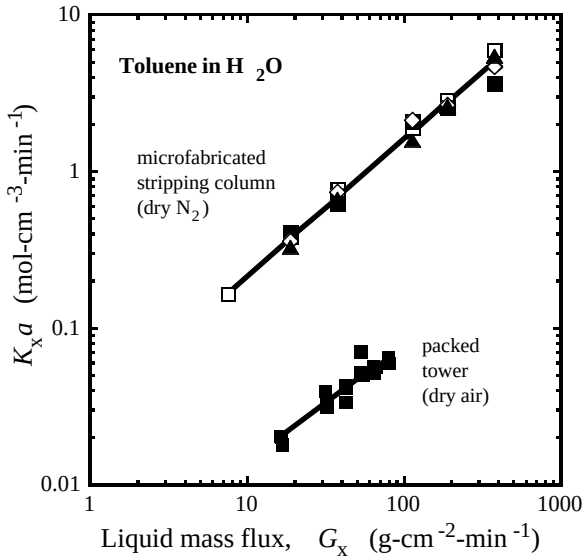

Fig. 6. Overall mass transfer capacity coefficient, $K_x a$, as a function of the liquid mass flux, G_x, for both the MFSC and the packed tower. The different symbols represent different values for the gas mass flux (for the MFSC).

seen there is only weak dependence implied between these quantities, and values for $\beta \sim 0.08$ and 0.12 for the MFSC and the packed tower, respectively, are found.

A final set of analyses was conducted to determine the best set of parameters, α, β and ψ that could describe each process. These results are shown in Table 1, where we also report the predicted values for each parameter based on the commonly used Onda et al. [14] and Sherwood and Holloway [15] correlations. The best fit parameters for Eq. (7) are shown in Table 1, along with 95% confidence intervals

Table 1
Calculated values for parameters in Eq. (7), along with predicted values based on previously published correlations [14,15]

Process/correlation	ψ	α	β
MFSC	0.026 ± 0.002	0.84 ± 0.06	0.08 ± 0.10
Packed tower	0.0024 ± 0.0002	0.72 ± 0.08	0.12 ± 0.04
Onda correlation[a]	N/A	0.67	0.00
Sherwood correlation[b]	N/A	0.70	0.00

All parameters are shown with 95% confidence intervals. ψ not given for either correlation since it is packing-dependent and is not applicable as a comparison to the MFSC.

[a] Assumes no resistance in the gas phase, and the wetted surface area of the packing remains constant.

[b] Assumes no resistance in the gas phase and 1 in. (25.4 mm) Pall rings are used.

for each value. We present another comparison between the experimental results and those predicted by Eq. (7) in Fig. 8. Here we plot the predicted values (based on the parameters and the values of G_x and G_y for each experiment) versus those measured experimentally. As may be seen for both the MFSC and the packed tower, essentially all of the results fall within a band given by 80–125% of the true value.

There are several major points to note from the results given in Table 1. First, the measured values for α for the packed tower are in very good agreement with both the Onda and Sherwood correlations. Second, there is negligible resistance to mass transfer in the gas phase, as revealed by β values near zero. This is expected when stripping volatile species with large Henry's constants, H. Inspection of Eq. (2) shows that a large value of H will result in K_x being dominated by mass transport in the liquid phase, k_x. This result has also been seen in previous work when stripping toluene from water using a packed tower [16]. Finally, the order of

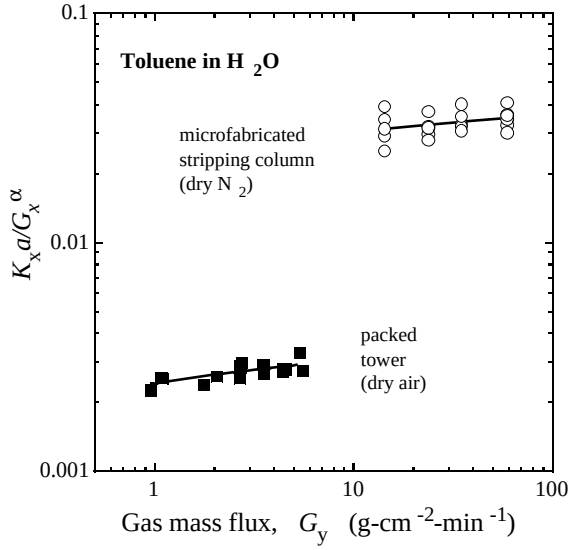

Fig. 7. The effect of the gas mass flux on the overall mass transfer capacity coefficient, $K_x a$. The dependence on the liquid mass flux has been removed using the results from Fig. 6, and the slope represents the parameter β for each case.

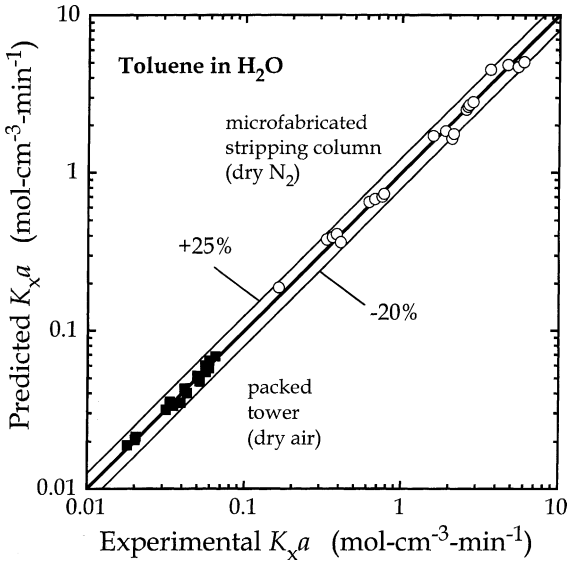

Fig. 8. Comparison of the experimentally measured and the values predicted by Eq. (7) for the overall mass transfer capacity coefficient, $K_x a$, for both the packed tower and the MFSC.

magnitude difference in the $K_x a$ values between the MFSC and packed tower is mostly reflected in the parameter ψ. Overall, the use of Eq. (7) along with the parameters given in Table 1, can predict the overall capacity coefficient for the toluene stripping process to within ±25% for both the MFSC and packed tower, as shown in Fig. 8. This is a reasonable amount of uncertainty and compares well to the error reported for the Onda correlation of ±20% [11].

Our results that show an order of magnitude difference between $K_x a$ for the MFSC and packed tower are significant since it shows that the MFSC can accomplish the same separation as the packed tower with several potential advantages: (1) the MFSC is approximately 10 times more volumetrically efficient than the packed tower; (2) there is no need for random or structured packing; (3) there is no chance for "flooding" to occur in the MFSC; and (4) the pressure drop is potentially lower over the MFSC as compared to the packed tower. Disadvantages of the MFSC probably include (1) manufacturing costs; (2) fouling of the perforations and/or microchannels; and (3) problems with scale-up or number-up strategies.

Focusing on performance issues, the interfacial area for mass transfer per volume, a, is $130\,m^2\,m^{-3}$ for the MFSC, while it is $200\,m^2\,m^{-3}$ [9] for 1.59 cm plastic Pall rings (this will decrease slightly when the packing is wet [14]). The value for a for the MFSC is an upper limit—only the volume of the Liquid-side microchannel was included in the calculation. Since the interfacial area per volume is nearly the same for both processes, it follows that most of the difference between $K_x a$ in the MFSC and packed tower is due to the overall mass transfer coefficient, K_x. Film theory states that the mass transfer coefficient through one phase, e.g., k_x for the liquid film, is proportional to D_{AB}/δ, where δ is the thickness of the film in that phase, and D_{AB} is the diffusivity [17]. In the MFSC, the liquid film thickness is intrinsic to the design and is simply equal to the height of the liquid channel, or 330 μm. To determine the thickness of the liquid film on the Pall rings in the packed tower, the average liquid velocity in the tower must be equated with the average velocity given by solving the Navier–Stokes Equation. The superficial velocities of gas and liquid are known for the packed tower from rotameter readings. The average velocity of liquid in the packed-region of the tower, $\langle v_L \rangle$, can be calculated using the following equation:

$$\langle v_L \rangle = \frac{U_0}{V_{f,L}} = \frac{U_0(Q_L + Q_G)}{\varepsilon Q_L} \tag{8}$$

This average velocity can be related to the liquid film thickness by finding the velocity profile in a falling film over the packing. Fig. 9 shows a schematic of the coordinate system used for this calculation. The Navier–Stokes equation simplifies to Eq. (9) for the geometry shown in Fig. 9, neglecting the curvature of the packing. The no-slip boundary condition at $y = 0$ is assumed, and therefore $v_x = 0$ at this point. Since we are interested in the smallest value for δ in the falling film, we want to know the thickness of the film just before flooding begins to occur. At this condition, the gas provides just enough shear stress on the liquid to have $v_x \to 0$ at $y = \delta$:

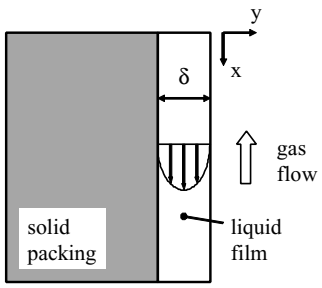

Fig. 9. Schematic of the coordinate system used to solve the Navier–Stokes equation for the velocity profile of a falling film.

$$\mu \frac{d^2 v_x}{dy^2} + \rho g = 0, \quad v_x = 0 \text{ at } y = 0 \text{ and } y = \delta \tag{9}$$

The solution to Eq. (9) is given by

$$v_x = \frac{\rho g}{2\mu}(\delta y - y^2) \tag{10}$$

The average velocity can then be calculated by integrating from 0 to δ and dividing by δ. The result is given as

$$\langle v_x \rangle = \frac{1}{\delta}\int_0^{\delta} \frac{\rho g}{2\mu}(\delta y - y^2)\,dy = \frac{\rho g \delta^2}{12\mu} \tag{11}$$

Eqs. (8) and (11) can be solved simultaneously to determine the liquid film thickness in the packed tower at flooding conditions. For the experiments that were close to flooding, it was observed that $Q_G \cong 100 Q_L$. The film thickness in the packed tower calculated for this near flooding condition is found to be 1050 μm, about three times that of the MFSC. Considering the assumptions that must be made to calculate the film thickness over the packing, this suggests that the order of magnitude increase of $K_x a$ in the MFSC is due primarily to the small liquid film thickness associated with this device. The film thicknesses obtainable with the MFSC are not feasible with traditional packed towers, even near flooding. As a comparison, it would take a liquid with a density similar to water but a viscosity an order of magnitude lower (such as benzene or another non-polar organic) in order to form a liquid film that compares in thickness to the MFSC. Liquids with higher viscosities would only increase the difference between the MFSC and the packed tower: an order of magnitude increase in viscosity (such as kerosene) causes the film thickness in the packed tower to increase by ~3 times. In addition, random packings do not wet homogeneously and poor contact with the stripping gas can result in inefficient separations, a problem not associated with the MFSC.

4. Conclusions

We have determined that a microfabricated stripping column possesses a higher volumetric efficiency as compared to a conventional packed column due to the higher obtainable values for the overall mass transfer coefficient in this device. The higher mass transfer coefficients in the MFSC can be attributed to the thin liquid film obtained in the device, a thickness that is unobtainable with traditional packed towers. Also, with a reduced possibility for "flooding" in the MFSC, any range of gas velocities can be employed and comparable decreases in VOC's can be obtained in a much smaller volume.

Acknowledgements

The authors wish to acknowledge the assistance and contributions of Mr. Aravind S. Killampalli and Mr. Todd W. Schroeder in certain aspects of the fabrication of the MFSC, and in the design of the microfluidic platform. We would also like to acknowledge the staff and the facilities at the Cornell NanoScale Science and Technology Facility, and the facilities of the Nanobiotechnology Center.

References

[1] H. Löwe, W. Ehrfeld, Electrochim. Acta 44 (1999) 3679–3689.
[2] K.F. Jensen, Chem. Eng. Sci. 56 (2001) 293–303.
[3] K. Jahnisch, M. Baerns, V. Hessel, W. Ehrfeld, V. Haverkamp, H. Lowe, Ch. Wille, A. Guber, J. Fluorine Chem. 105 (2000) 117–128.
[4] R. Chambers, R. Spink, Chem. Commun. 10 (1999) 883–884.
[5] T. Cui, J. Fang, A. Zheng, F. Jones, A. Reppond, Sens. Actuators B 71 (2000) 228–231.
[6] C. Turner, J. Shaw, B. Miller, V. Bains, in: I. Renard (Ed.), Proceedings of the Fourth International Conference on Microreaction Technology (iMRET-4), 2000, pp. 106–113.
[7] W. TeGrotenhuis, R. Cameron, V. Viswanathan, R. Wegeng, in: W. Ehrfeld (Ed.), Proceedings of the Third International Conference on Microreaction Technology (iMRET-3), 1999, pp. 541–549.
[8] International Critical Tables of Numerical Data, Physics, Chemistry and Technology, First Electronic Edition, vol. III, Knovel, New York, 2003, p. 391.
[9] J. Seader, E. Henley, Separation Process Principles, 3rd ed., 1998, pp. 317–342.
[10] W. McCabe, J. Smith, P. Harriott, Unit Operations of Chemical Engineering, McGraw-Hill, Boston, 2001, pp. 689–713.
[11] Y. Djebbar, R. Narbaitz, Water Sci. Technol. 38 (1998) 295–302.
[12] S. Piche, B. Grandjean, I. Iliuta, F. Larachi, Environ. Sci. Technol. 35 (2001) 4817–4822.
[13] Y. Djebbar, R. Narbaitz, Can. J. Civil Eng. 23 (1996) 549–559.
[14] K. Onda, H. Takeuchi, Y. Okumoto, J. Chem. Eng. Jpn. 1 (1968) 56–62.
[15] T. Sherwood, F. Holloway, Trans. AIChE 36 (1940) 39.
[16] J. Ortiz-Del Castillo, G. Guerrero-Medina, J. Lopez-Toledo, J. Rocha, Ind. Eng. Chem. Res. 39 (2000) 731–739.
[17] J. Welty, Fundamentals of Momentum, Heat, and Mass Transfer, 4th ed., Wiley, New York, 2001, pp. 645–681.